

The Eosin-5-maleimide Binding Site on Human Erythrocyte Band 3: Investigation of Membrane Sidedness and Location of Charged Residues by Triplet State Quenching[†]

Rui-jun Pan and Richard J. Cherry*

Department of Biological Sciences, Central Campus, University of Essex, Wivenhoe Park, Colchester, CO4 3SQ, U.K.

Received February 16, 1998; Revised Manuscript Received April 30, 1998

ABSTRACT: The triplet probe eosin-5-maleimide (EMA) is a specific inhibitor of anion transport mediated by the erythrocyte membrane protein, band 3. It was previously shown that the eosin moiety is located close to the anion binding site when EMA is covalently bound to band 3 [Pan, R.-j., and Cherry, R. J. (1995) *Biochemistry* 34, 4880–4888]. In the present study the electrostatic properties and membrane sidedness of the EMA binding site of band 3 were further investigated by triplet state quenching. A series of stable nitroxyl free radicals, which are characterized by different charges, and I^- were used as the quenchers. Time-resolved laser spectroscopy was employed to measure the triplet lifetime of EMA. It was found that the quenching reaction between the quenchers and band 3-bound EMA follows a linear Stern–Volmer plot. The quenching rate constants (K_q) of the quenchers are in the order of NH_3^+ -TEMPO ($K_q = 6.34 \times 10^6 \text{ M}^{-1} \text{ s}^{-1}$) > TEMPO-Choline⁺ ($K_q = 2.18 \times 10^6 \text{ M}^{-1} \text{ s}^{-1}$) > TEMPO ($K_q = 1.13 \times 10^6 \text{ M}^{-1} \text{ s}^{-1}$) > I^- ($K_q = 2.46 \times 10^5 \text{ M}^{-1} \text{ s}^{-1}$) > pyrroline-COO[−] ($K_q = 2.18 \times 10^4 \text{ M}^{-1} \text{ s}^{-1}$). Experiments with resealed ghosts and inside-out vesicles revealed that negatively charged quenchers can only access the EMA binding site from the extracellular side of the membrane while the positively charged quenchers acted from the cytoplasmic side. The ionic strength dependence of the quenching rate constants and the effects of pH on the quenching reaction were also studied. For both TEMPO-Choline⁺ and I^- , the K_q values decreased as the ionic strength increased, but quenching by TEMPO was independent of the ionic strength variation over the same range. It was also found that at lower pH, the I^- quenching rate constant increases but the TEMPO-choline⁺ quenching rate constant decreases. In both cases, the dependence of quenching on pH exhibited an apparent pK_a of about 6.5, which suggests the involvement of one or more histidine residues. This notion gained further support from the finding that modification of His residues of band 3 by DEPC reduced I^- quenching at pH 6. On the basis of these results, it is proposed that eosin is located in the anion transport channel such that it is accessible from both sides of the membrane. Histidine residues, which have previously been proposed to lie in the anion channel, probably are located on either side of the eosin probe where they contribute to electrostatic interactions which determine the K_q values for the charged quenchers.

To meet the need for rapid HCO_3^- and Cl^- exchange, the erythrocyte membrane contains a large number of copies of the anion exchanger, band 3 ($\sim 10^6$ copies per cell). The band 3 polypeptide can be structurally and functionally divided into two distinct domains. The 43 kDa hydrophilic cytoplasmic domain of band 3 provides binding sites for the membrane cytoskeletal proteins, hemoglobin, and some glycolytic enzymes (1). The 52 kDa membrane-spanning domain executes the anion transport function and is believed to span the bilayer up to 14 times in the form of α -helices (2–6).

Several classes of probes have been applied to investigate band 3 structure and function. Eosin derivatives have been shown to inhibit the transport activity by binding to band 3 either covalently or noncovalently (7, 8). Macara et al. (9) localized the site of eosin-5-maleimide (EMA)¹ labeling to a 17 kDa fragment of the membrane domain of band 3.

Because there is only one cysteine residue (Cys-479) in this 17 kDa fragment, it was thought that Cys-479 was likely to be the EMA covalent labeling site on the basis of the preferential chemical reactivity of maleimide with SH groups (10). However, later studies demonstrated that Lys-430 is the residue with which EMA covalently reacts (11, 12). It is unlikely that Lys-430 is directly included in the transport site because (a) site-directed mutation of Lys-430 did not

¹ Abbreviations: EMA, eosin-5-maleimide; B3-EMA, EMA bound to band 3; CHES, 2-[N-cyclohexylamino]ethanesulfonic acid; DEPC, diethyl pyrocarbonate; DIDS, 4,4'-diisothiocyanatostilbene-2,2'-disulfonic acid disodium salt; HEPES, 2-[N-hydroxyethyl]piperazine-N'-2-ethanesulfonic acid; IOVs, inside-out vesicles; TEMPO, 2,2,6,6-tetramethylpiperidine-N-oxyl; TEMPO-Choline⁺, 4-(N,N-dimethyl-N-(2-hydroxyl)-2,2,6,6-tetramethylpiperidine-N-oxyl; NH_3^+ -TEMPO, 4-amino-2,2,6,6-tetramethylpiperidine-N-oxyl; PMSF, phenylmethanesulfonyl fluoride; 5PB, 5 mM sodium phosphate buffer, pH 7.8; PBS, 5 mM sodium phosphate, 150 mM NaCl, 1 mM EDTA, pH 7.8; RSGs, resealed right-side-out ghosts; SDS–PAGE, sodium dodecyl sulfate–polyacrylamide gel electrophoresis; 310 Buffer, 90 mM disodium hydrogen phosphate, 20 mM sodium dihydrogen phosphate, pH 7.5.

[†] Supported by the Wellcome Trust and BBSRC.

* Author to whom correspondence should be addressed.

alter band 3 mediated anion exchange (12), (b) Lys-430 is located at the border between the first transmembrane helix and the first extracellular loop from the N-terminus of the protein, but it is generally accepted that the transport site could be some distance from the surface of the membrane (13, 14), (c) mutation of Lys-449 in mouse (equivalent to Lys-430 in human) only abolishes the EMA irreversible reaction. The EMA reversible inhibition of anion transport still occurs (15). Therefore, residues that are close to the eosin moiety could play a more important role in the anion exchange.

Recently, we have studied fluorescence quenching of band 3-bound eosin-5-maleimide (B3-EMA) by the transportable substrate I^- (16). We observed nonlinear Stern–Volmer plots which were interpreted by a binding-diffusion model in which quenching is determined by binding of I^- to a site in close proximity to the eosin probe. By determining the dissociation constant for I^- and for other transportable anions which competed for the same site, we concluded that the site is very probably the anion transport site on band 3. We proposed that EMA is located in the wall of an access channel on the extracellular side of the membrane where it inhibits anion translocation but not anion binding. Knauf and co-workers also find that EMA does not inhibit anion binding but the location of EMA is disputed (8, 17, 18).

Macara et al. (9) observed that B3-EMA is only accessible to the fluorescence quencher, Cs^+ , from the cytoplasmic side of the membrane. In contrast, Wyatt and Cherry (19) found that I^- quenches the eosin triplet state only from the extracellular side of the membrane. The reason for the different sidedness of these quenching reactions is unclear. Because of its long lifetime (~ 2 ms), the triplet state of eosin is very sensitive to quenching reactions, thus permitting a wider range of quenchers to be investigated than is the case for fluorescence quenching. In the present study, a series of triplet quenchers are used to investigate the microenvironment around the EMA binding site on band 3. These studies show that positively and negatively charged quenchers act from opposite sides of the membrane and that histidine residues, which are probably within the anion transport pathway, are located close to the eosin probe. The data provide further evidence for a close spatial relationship between the eosin probe and the anion transport pathway of band 3.

MATERIALS AND METHODS

EMA, TEMPO-choline⁺ and pyrroline-COO⁻ were obtained from Molecular Probes Inc. TEMPO, NH_3^+ -TEMPO, DEPC, neuraminidase type VI (from *Clostridium perfringens*), trypsin (from bovine pancreas), and Dextran T-110 were from Sigma. All other reagents used were of the highest grade available.

Preparation of Resealed Ghosts (RSGs) with Quencher I^- Inside. Band 3 was selectively labeled with EMA by incubating intact erythrocytes from fresh human blood with EMA as described by Nigg and Cherry (7). The red blood cells were washed three times with PBS, then hemolyzed in 20 vol of 5PB. The resealing of EMA-labeled ghosts was accomplished as described by Wyatt and Cherry (19) with some modification. Briefly, the unsealed EMA-labeled ghosts were incubated at 37 °C for 45 min in the dark, with

occasional agitation of the solution. The incubation buffer contained 5 mM HEPES, 28 mM trisodium citrate, 1 mM $MgSO_4$, and 10 mM KI, pH 7.8. Then the I^- -entrapped RSGs were collected by centrifugation at 30000g for 10 min at 4 °C and washed three times in 5 mM HEPES, 28 mM trisodium citrate, and 10 mM KCl, pH 7.8. For the control RSGs, the same preparation was performed except that the incubation buffer contained 10 mM KCl rather than 10 mM KI.

The concentration of the entrapped I^- was measured on an ion exchange apparatus, Dionex 2000i/SP (Dionex (UK) Ltd. Surrey, U.K.). Briefly, aliquots of standard KI solutions in 5 mM HEPES, 28 mM trisodium citrate, and 0.5% Triton X-100, pH 7.8, were applied to the instrument to identify the I^- elution peak. A plot of the I^- elution peak area values against a series of known I^- concentrations was used as a calibration curve. To determine the entrapped I^- concentration, 500 μ L of resealed ghost pellet was dissolved with 500 μ L of 1% Triton X-100, 5 mM HEPES, 28 mM trisodium citrate, pH 7.8, and the sample solution applied to the instrument. To determine I^- retention over the time required for fluorescence quenching experiments (~ 2 h), RSGs were suspended in 5PB for different times at 37 °C and centrifuged prior to assaying for I^- . In a control experiment, no I^- was detected if the identical procedure was followed with unsealed ghosts, demonstrating that there was no interference to the assay from the erythrocyte membranes.

Preparation of Inside-Out Vesicles (IOVs). Inside-out vesicles (IOVs) were prepared as described by Steck and Kant (20). In brief, unsealed EMA-labeled ghosts were resuspended in 0.5 mM phosphate buffer, pH 7, containing 0.5 mM EGTA by vigorous mixing. The membrane suspension was incubated for 15 min at 35 °C, and then passed through a no. 27 gauge needle 5 times to complete vesiculation. The resultant membrane vesicles were centrifuged at 27000g for 20 min at 4 °C to pellet the membranes. Sealed IOVs were separated from unsealed membranes and right-side-out vesicles by the following protocol. The pellet homogenates were diluted 4 times in 5PB and layered upon an equal volume of a dextran barrier solution (4% Dextran T-110 (w/v) in 5PB, pH 7.8; density 1.03 mg/mL) in a centrifuge tube. The sample was centrifuged for 30 min at 30000g at 4 °C which resolved the sample into a pellet at the bottom and a band floating on the top of the dextran barrier. The pellet, containing unsealed membrane fragments and right-side-out vesicles, was discarded. IOVs were harvested in the band on the top of the dextran barrier and washed again with 5PB by centrifugation at 28000g for 30 min.

Sidedness and resealing efficiencies of IOVs were determined from the latency of neuraminic acid accessibility to neuraminidase (9, 20). Briefly, aliquots of IOV suspensions at concentration of 2–4 mg of protein per mL in 5PB pH 7.8 were incubated at 20 °C for 30 min with an equal volume of 0.1 mg/mL neuraminidase solution in 0.1 M Tris-HCl buffer, pH 5.7, with or without 0.2% Triton X-100. The sialic acid released was determined directly by the thiobarbituric acid assay as described by Warren (21). The assay was carried out by following procedures: (1) To 0.2 mL of neuraminidase-treated membrane solution was added a volume of 0.1 mL of the solution containing 0.2 M sodium metaperiodate 53% (v/v) phosphoric acid. The solution was

thoroughly mixed and incubated at 20 °C for 20 min. (2) One milliliter of 10% sodium arsenate in 0.5 M sodium sulfate solution was added and vigorously vortexed. (3) Three milliliters of 0.6% 2-thiobarbituric acid (w/v) in 0.5 M sodium sulfate solution was added and the contents were incubated in a boiling water bath for exactly 15 min. (4) After cooling, 4 mL of cyclohexane was added to the sample tubes and the contents were then vigorously shaken several times. Red color products, distributed in the cyclohexane phase, were collected (5). The extinction coefficient of 57000 M⁻¹ cm⁻¹ at wavelength of 549 nm was used to determine *N*-acetylneuraminic acid concentration. IOVs treated with neuraminidase in the presence of 0.2% Triton X-100 were taken as the control for the 100% permeable membranes. IOV preparations of less than 85% resealing efficiencies were discarded.

Ionic Strength. The ionic strength of membrane samples in 5PB was varied by adding different amounts of trisodium citrate. The pH value of the buffers was adjusted to 7.8. In some experiments with I⁻ as quencher, glycylglycine was used instead of citrate; similar results were obtained with either of these anions.

pH Titration and DEPC Modification of EMA-Labeled Ghosts. The buffers used in the pH titration experiments were prepared as follows: the buffer with pH < 6.5 contained 5 mM MES, the buffers with pH between 6.5 and 8.0 contained 5 mM HEPES, and the buffer of pH 8.5 contained 5 mM CHES. All of the buffers were adjusted to the indicated pH values by either 1M HCl or 1 M NaOH.

Modification of the membrane protein by DEPC was carried out as described by Izuahara et al. (22). The EMA-prelabeled unsealed ghosts were incubated for 30 min at 0 °C with freshly prepared 5 mM DEPC in 5 mM HEPES, pH 7.8. The DEPC modified ghosts were subsequently washed three times with 5PB.

The p*K*_a of the acidic group of eosin in B3-EMA was determined by fluorescence methods. Briefly, EMA-labeled ghosts were suspended in 5 mM MES. The pH of the sample buffer was varied by 0.1 M HCl or 0.1 M NaOH, and a plot of fluorescence intensity against pH was obtained.

Cleavage of the Cytoplasmic Domain of Band 3 with Trypsin. Removal of the cytoplasmic domain of band 3 by trypsin was carried out as described by Nigg and Cherry (23). The EMA-labeled ghosts, at ~2 mg of protein/mL, were incubated with 2 μg/mL trypsin in 5PB for 1 h at room temperature. To stop the reaction, ice-cold 5PB containing 0.5 mM PMSF was added. Ten percent SDS-PAGE was used to check the removal of the cytoplasmic domain of band 3.

Triplet State Lifetime and Transient Dichroism Measurements. The apparatus used for measuring the triplet lifetime and dichroism of transient absorbance changes was similar to that described in detail elsewhere (24). A Nd-YAG laser (JK Laser, Ltd.) was used to excite the probe. A frequency doubler converted the wavelength to 532 nm. The pulse width was about 15 ns, and the repetition rate was 10 Hz. Transient absorbance changes at time *t* after the flash arising from the probe molecule ground-state depletion were simultaneously recorded at 515 nm for light polarized parallel (*A*_∥(*t*)) and perpendicular (*A*_⊥(*t*)) with respect to the polarization of the exciting laser flash beam. Up to 512 signals were averaged in a Datalab DL 102A signal averager.

The total absorbance change *A*(*t*) is proportional to the population of probe molecules in the triplet state and is given by

$$A(t) = A_{\parallel}(t) + 2A_{\perp}(t) \quad (1)$$

The triplet lifetime was determined by fitting *A*(*t*) to the equation

$$A(t) = A_1 \exp(-t/\tau_1) + A_2 \exp(-t/\tau_2) \quad (2)$$

using a nonlinear least-squares program. The mean triplet lifetime, τ , was determined from the best-fit values of τ_1 and τ_2 according to

$$\tau = (A_1\tau_1 + A_2\tau_2)/(A_1 + A_2) \quad (3)$$

Values of τ were then obtained by averaging results from 3 different samples.

All samples were flushed with argon to remove oxygen which quenches the probe triplet state. It was noted that in the RSG and IOV preparations, it is more difficult to remove oxygen from the sample. This problem was solved by bubbling the sample with argon for 2 min and sealing the sample cell in the dark for 5 min to allow equilibration with oxygen remaining in the cell. This procedure was then repeated five times. The sample concentration was typically adjusted to ~2 μM with respect to EMA and the measurements were made at 37 °C.

The effect of the quenchers on the triplet lifetime was analyzed by the Stern–Volmer equation (25):

$$\tau_0/\tau = 1 + K_q\tau_0[Q] \quad (4)$$

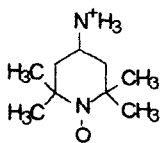
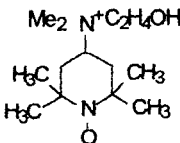
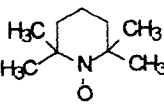
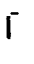
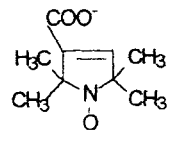
where τ_0 is the triplet lifetime in the absence of quencher, K_q is the dynamic quenching constant, and [Q] is the quencher concentration. The quenching experiments were performed with varying concentrations of the quenchers present in the membrane suspension medium. In the case of I⁻ quenching experiments, the ionic strength was maintained at 20 mM by compensation with trisodium citrate.

RESULTS AND ANALYSIS

Characteristic of Triplet State Quenching of EMA-Band 3 in Unsealed Ghosts by Different Quenchers. Figures 1–3 show that the triplet state lifetime of band 3-bound EMA becomes shorter with increasing concentration of the quenchers I⁻, NH₃⁺-TEMPO, and TEMPO. There is no significant difference in the initial absorbance change demonstrating that the quenching reactions are dynamic in all cases. The corresponding Stern–Volmer plots are linear as is also expected for dynamic quenching. Similar results were obtained for quenching experiments performed with the spin labels, TEMPO-choline⁺ and pyrroline-COO⁻.

The structures of the different quenchers used in the present work together with their corresponding quenching rate constants are presented in Table 1. The p*K*_a value for NH₃⁺-TEMPO is 9.6, and for pyrroline-COO⁻ the p*K*_a is 3.2 (26). At pH 7.8, pyrroline-COO⁻ and I⁻ are negatively charged, NH₃⁺-TEMPO and TEMPO-choline⁺ are positively charged, and TEMPO is uncharged. Thus these quenchers provide a convenient series to study the electrostatic properties of the EMA binding site on band 3. The quenching

Table 1: The Triplet State Quenchers and Their Quenching Rate Constant for EMA-Labeled Unsealed Ghosts^a

Quencher	NH ₃ ⁺ -TEMPO	TEMPO-Choline ⁺	TEMPO	Iodide	Pyrroline-COO ⁻
Structure					
pK _a	9.6	>10			3.2
K _q (M ⁻¹ s ⁻¹)*	6.34 X 10 ⁶	2.18 X 10 ⁶	1.13 X 10 ⁶	2.46 X 10 ⁵	5.35 X 10 ⁴

^a The quenching experiments were performed in 5PB, pH 7.8, at 37 °C. K_q values were calculated from the slopes of the linear Stern–Volmer plots as described in Materials and Methods.

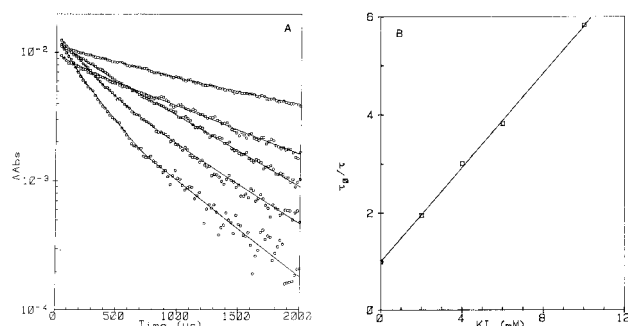
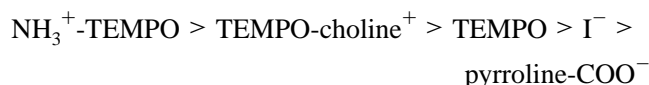


FIGURE 1: Triplet state quenching of B3-EMA by I⁻. The EMA-labeled unsealed ghosts were in 5PB, pH 7.8. The ionic strength of the quenching buffer was maintained at 20 mM by trisodium citrate. The temperature was 37 °C. (A) Triplet state decays fitted to the data by eq 2 as described in Materials and Methods. From top to bottom [I⁻] = 0, 2.0, 4.0, 6.0, and 10 mM. (B) Stern–Volmer plot of mean triplet lifetimes from data in (A).

efficiencies of the quenchers were found to be in the following order:



The Sidedness of the Quenching Reaction Is Dependent on Charge on the Quencher. To investigate the membrane sidedness of the quenching reactions between the quenchers and B3-EMA, the quenching experiments were performed in RSGs and IOVs. It was previously established that the erythrocyte membranes are impermeable to charged spin label compounds such as TEMPO-choline⁺ (27), NH₃⁺-TEMPO, and pyrroline-COO⁻ (26).

Figure 4(A) and Table 2 show the effect of 0.8 mM TEMPO on the triplet lifetimes of B3-EMA for unsealed ghosts, RSGs, and IOVs. The calculated mean triplet lifetimes are 729(±38) μs, 746(±51) μs, and 759(±44) μs, respectively, demonstrating that the TEMPO quenching reaction is independent of the sidedness of the membrane (the small differences in initial absorbance change are due to sample variability). These results are expected because, as a hydrophobic compound, TEMPO can freely diffuse across the erythrocyte membrane lipid bilayer (28). They also exclude the possibility that vesiculation and resealing of the membrane preparations may alter the conformation of band 3.

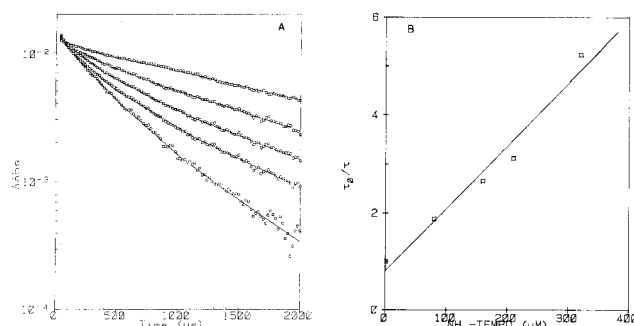


FIGURE 2: Triplet state quenching of B3-EMA by NH₃⁺-TEMPO. Experimental details as in Figure 1. (A) Triplet state decays fitted to the data by eq 2 as described in Materials and Methods. From top to bottom [NH₃⁺-TEMPO] = 0, 0.08, 0.16, 0.20, and 0.32 mM. (B) Stern–Volmer plot of mean triplet lifetimes from data in (A).

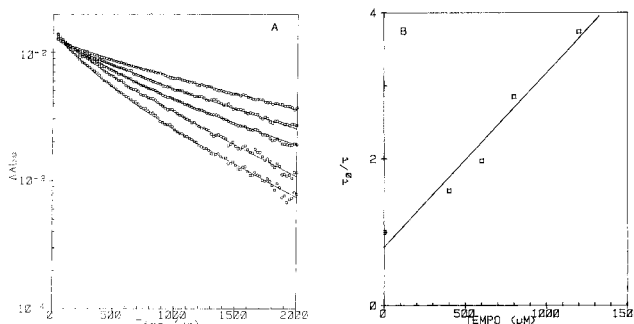


FIGURE 3: Triplet state quenching of B3-EMA by TEMPO. Experimental details as in Figure 1. (A) Triplet state decays fitted to the data by eq 2 as described in Materials and Methods. From top to bottom [TEMPO] = 0, 0.4, 0.6, 0.8, and 1.2 mM. (B) Stern–Volmer plot of mean triplet lifetimes from data in (A).

For the charged quenchers, however, the quenching efficiencies are dependent on the membrane preparations (Figure 4B,C and Table 2). In the presence of the negatively charged quenchers, the mean triplet lifetime is similar in unsealed ghosts and in RSGs, whereas in IOVs the lifetime is similar to the control (no quencher present). The somewhat shorter mean lifetime recorded for IOVs in the presence of the negatively charged quenchers is accounted for by the fact that up to 15% of IOVs may be unsealed as judged by the neuraminidase assay.

In addition, the experiment of resealing I⁻ into the RSGs (19) was repeated. After washing the I⁻-entrapped RSGs

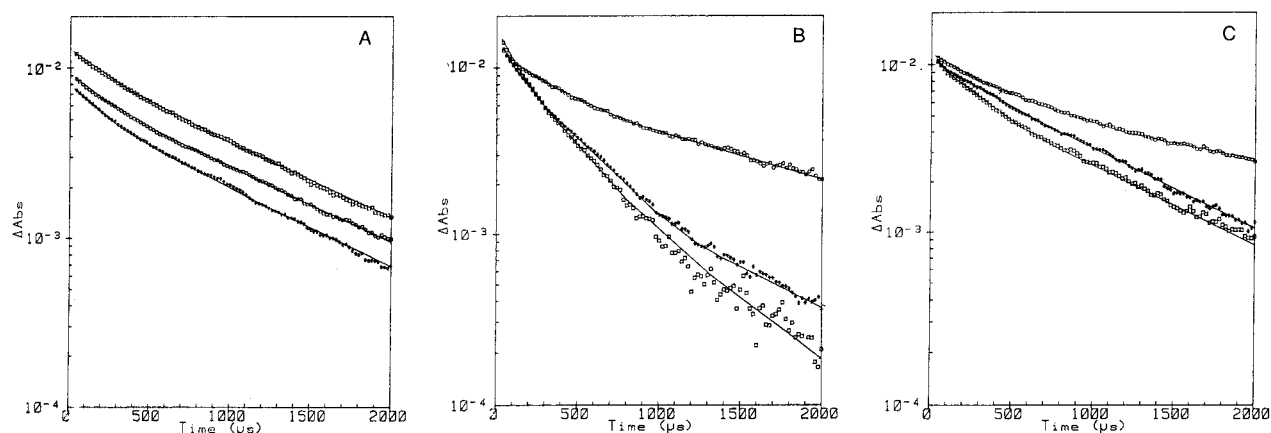


FIGURE 4: Sidedness effects on the quenching reaction between B3-EMA and the triplet state quenchers. All samples were in 5PB buffer containing 28 mM trisodium citrate, pH 7.8. The temperature was 37 °C. (A) Quenching of B3-EMA by TEMPO: In the presence of 0.8 mM TEMPO, the mean triplet lifetimes are 746(±37) μ s for RSGs (□); 729(±41) μ s for EMA-labeled unsealed ghosts (*), and 759(±47) μ s for IOVs (○). (B) Quenching of B3-EMA by TEMPO-choline⁺: In the presence of 0.7 mM TEMPO-choline⁺ the mean triplet lifetimes are 968(±31) μ s for RSGs (○), 324(±36) μ s for EMA-labeled unsealed ghosts (□); and 452(±43) μ s for IOVs (*). (C) Quenching of B3-EMA by pyrroline-COO⁻: In the presence of 25 mM pyrroline-COO⁻, the mean triplet lifetimes are 756(±43) μ s for RSGs (□), 814(±34) μ s for EMA-labeled unsealed ghosts (*), and 1410(±54) μ s for IOVs (○).

Table 2. Sidedness Effects on the Triplet Quenching Reaction^a

quencher	mean triplet Lifetime (μ s)		
	unsealed ghosts	RSGs	IOVs
TEMPO (0.8 mM)	729(±38)	746(±51)	759(±44)
TEMPO-choline ⁺ (0.8 mM)	452(±43)	968(±31)	324(±36)
NH ₃ ⁺ -TEMPO (0.3 mM)	493(±36)	829(±26)	426(±41)
KI (8.0 mM)	589(±38)	675(±47)	1328(±54)
pyrroline-COO ⁻ (25 mM)	814(±34)	759(±43)	1410(±54)
no quencher	1804(±96)	1740(±85)	1760(±67)

^a Values are mean (±SD) of three determinations.

several times with the I⁻-free buffer, the concentration of the RSG-entrapped I⁻ in this experiment was measured to be 8 mM which is 80% of the I⁻ concentration present in the resealing buffer. This I⁻ concentration was maintained for at least 3 h, no doubt due to inhibition of anion transport by bound EMA (7). It is expected that had B3-EMA been accessible to I⁻ from the cytoplasmic side of the membrane, then in the presence of 8 mM I⁻ the triplet lifetime would have been about 400 μ s (see Figure 1 (A)). However, the triplet lifetime of B3-EMA was found to be about 1800 μ s in this experiment, which is very close to the triplet lifetime in the absence of quencher. Thus it may be concluded that the eosin probe is only accessible to the negatively charged quenchers from the extracellular side of the membrane.

In the presence of the positively charged quenchers, NH₃⁺-TEMPO and TEMPO-choline⁺, the mean triplet lifetime is similar in unsealed ghosts and IOVs, suggesting that these quenchers access the eosin probe from the cytoplasmic side of the membrane. A complication in this case is that the mean lifetime in RSGs, although longer than in unsealed ghosts and IOVs, is much shorter than in the control. An explanation of this observation is suggested by considering the separate lifetimes τ_1 and τ_2 which are used to calculate the mean lifetime. For RSGs in the presence of the positively charged quenchers, the triplet decay consists of a long-lived component (60%) with lifetime similar to that of the control and a short-lived component (40%) with a lifetime of a few hundred microseconds [in the control, the long-lived component (τ_2 = ~1.9 ms) comprises 92% of the decay]. This strongly suggests that a rather high fraction of the RSGs are

leaky to the quenchers and give rise to the short-lived component which reduces the value of the mean lifetime. Assays of the extent of resealing showed that 20–30% of iodide is lost from RSGs, in support of the above explanation. A previous determination using a fluorescence assay indicated a similar extent of resealing (19). It should be noted that the long-lived component is completely absent when positively charged quenchers are added to unsealed ghosts or to IOVs. Overall, the data thus imply that the positively charged quenchers access the eosin probe preferentially, and very probably exclusively, from the cytoplasmic side of the membrane.

An alternative explanation of quenching by the cationic quenchers is that they bind to the cytoplasmic-facing side of band 3 and induce internal quenching of fluorescence via a conformational change. This, however, seems highly unlikely since there is no evidence that the large changes in triplet lifetime observed in these experiments can arise from a conformational change. Moreover, a mechanism involving binding would be saturable and give rise to downward curving Stern–Volmer plots (16).

Dependence of K_q on the Ionic Strength. From the above results, it appears that when covalently bound to band 3, the eosin moiety is extracellularly accessible to the negatively charged quenchers and intracellularly accessible to the positively charged quenchers. These effects are most likely to arise from charged residues in the vicinity of the EMA probe. To investigate electrostatic properties of the quenching reactions, the dependence of the quenching efficiencies on the ionic strength was studied. The basis for this approach is that the apparent quenching rate constant, K_q , of a charged quencher is determined by (25)

$$K_q = A \exp(BZ_q Z_m \sqrt{\mu}) \quad (5)$$

where A and B are constants, Z_q is charge of the quencher, Z_m is the charge of the probe binding site, and μ is the ionic strength. From eq 5, it is predicted that if Z_q and Z_m are the same sign, increasing μ will lead to increasing K_q . On the other hand, if Z_q and Z_m are of opposite sign, increasing μ will lead to decreasing K_q .

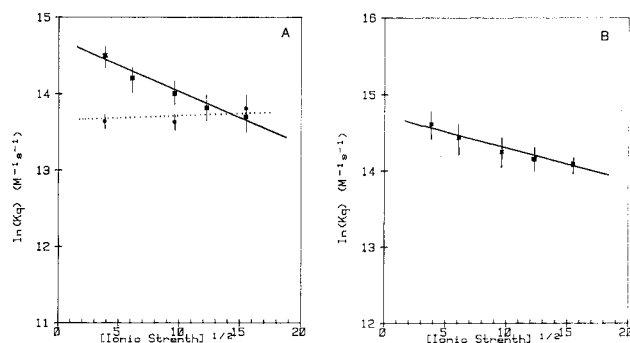


FIGURE 5: Ionic strength dependence of the quenching rate constant (K_q) for neutral and differently charged quenchers. EMA-labeled unsealed ghosts were in 5PB buffer and the temperature was 37 °C. The ionic strength was adjusted by trisodium citrate as indicated. (A) TEMPO-choline⁺ (■, solid line), TEMPO (●, dotted line). (B) I⁻.

In EMA-labeled unsealed ghosts, the K_q value for TEMPO is independent of the ionic strength (Figure 5A), as expected for an uncharged quencher. This result implies that the conformation of EMA-labeled band 3 is not altered within the citrate concentration range used. However, the K_q values for TEMPO-choline⁺ and I⁻ were both decreased as the ionic strength increased. Plots of $\log K_q$ against $\sqrt{\mu}$ are approximately linear as predicted by eq 5 (Figure 5A,B). These results clearly indicate that Z_m is positive for negatively charged quenchers and negative for positively charged quenchers. This is only possible if the negatively and positively charged quenchers approach the eosin moiety by different routes, in agreement with the sidedness of the quenching reactions. It appears that Z_m is negative on the cytoplasmic side and positive on the extracellular side of the membrane.

pH Dependence of the Quenching Reactions. Figure 6A shows that K_q values for I⁻ decrease as the pH rises from 5.5 to 8.5, consistent with the result of a previous study (19). The pH titration profile is characterized by an apparent pK_a value of ~6.5. The pH dependence of the quenching rate constant could originate from either an overall band 3 conformational change or from protonation and deprotonation of ionizable group(s) close to the EMA binding site. Quenching of band 3-bound EMA by TEMPO, however, is insensitive to pH (Figure 6B), suggesting that the conformation of band 3 is unlikely to change within the pH range of the experiment. Furthermore, quenching by TEMPO-choline⁺ is enhanced as the pH rises, with the same apparent pK_a value (~6.5) as for I⁻ (Figure 6B).

It was previously established that the conformation of the cytoplasmic domain of band 3 is strongly dependent on the pH in a range similar to that used in the present study (1). To see whether the cytoplasmic domain of band 3 also contributes to the pH effects on the quenching reaction, this domain was removed by mild trypsin proteolysis. The removal of the cytoplasmic domain was confirmed by SDS-PAGE and by the increased rotational mobility (29) of the membrane domain of EMA-labeled band 3 (data not shown). From Figure 6C,D, it is clear that truncating the cytoplasmic domain of band 3 did not change the pH titration profiles for quenching of B3-EMA by I⁻ and TEMPO-choline⁺. The quenching by TEMPO was also independent of the cytoplasmic domain.

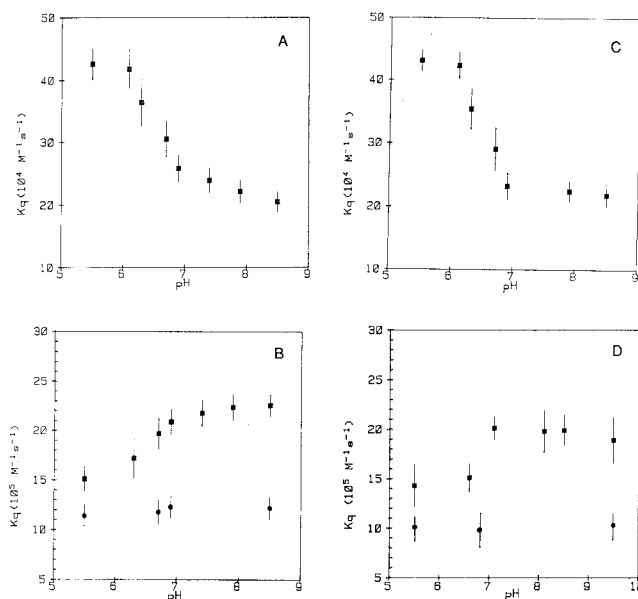


FIGURE 6: pH dependence of the quenching reactions between different quenchers and B3-EMA in unsealed ghosts and trypsinized ghosts. MES buffer (5 mM) was used for the pH range of 5.5–6.3, 5 mM HEPES buffer for the pH range of 6.7–7.9, and 5 mM CHES buffer was used for pH 8.5. Removal of the cytoplasmic domain of band 3 by trypsin was as described in the Materials and Methods. (A) Quenching of B3-EMA by I⁻ in unsealed ghosts. (B) Quenching of B3-EMA by TEMPO (●) and TEMPO-choline⁺ (■) in unsealed ghosts. (C) Quenching of B3-EMA by I⁻ in trypsinized ghosts. (D) Quenching of B3-EMA by TEMPO (●) and TEMPO-choline⁺ (■) in trypsinized ghosts.

Effect of DEPC Modification on the Quenching Reactions. It is unlikely that the proposed ionizable group(s) is on the eosin moiety since it was previously reported that quenching of free EMA by I⁻ is independent of pH in the same range as that applied in the present study (19). We also determined that the apparent pK_a of the acidic groups on the eosin moiety of B3-EMA is about pH 4.5. It is known that the typical pK_a of the imidazole group of histidine is about pH 6.5, which is very close to that observed in the present pH titration. This prompts the speculation that the histidine residue(s) may be the relevant ionizable group(s) which is close to the EMA binding site. To investigate the possible participation of histidine residues, we examined the effect of DEPC modification of band 3 on the I⁻ quenching reaction at pH 6 and pH 8.5, respectively. As shown in Figure 7A, at pH 6, the quenching of DEPC-modified B3-EMA by I⁻ is much less efficient than that of unmodified B3-EMA. At pH 8.5, however, quenching by I⁻ did not show any significant difference between DEPC-modified B3-EMA and unmodified B3-EMA (Figure 7B). It was also found that at pH 6 quenching by TEMPO was unchanged upon DEPC modification (Figure 7C).

DISCUSSION

It has long been known that the band 3 protein mediates essentially electrically silent anion exchange. However, electrostatic interactions between a substrate anion and the transport domain of band 3 were suggested to be involved in the mechanism of the anion transport process (13). Therefore, the study of the electrostatic properties of the anion transport channel is of considerable interest. Recently, a 20 nm structural model obtained from two-dimensional

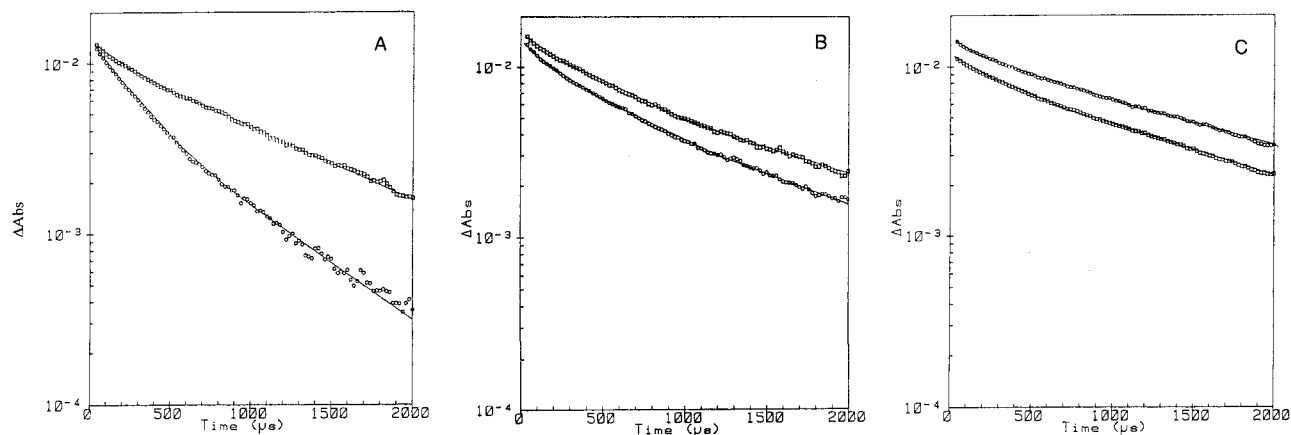


FIGURE 7: Effect of DEPC modification on the decay of the triplet state of B3-EMA in the presence of different quenchers at different pH. (A) Quenching of DEPC-modified ghosts by I^- at pH 6.0. The sample was in 5 mM MES buffer, pH 6.0, containing 3 mM KI. The temperature was 37 °C. (□) DEPC-modified EMA-labeled ghosts, mean triplet lifetime of $1196(\pm 36)$ μ s; (○) control EMA-labeled ghosts, mean triplet lifetime of $512(\pm 45)$ μ s. (B) Quenching of DEPC-modified ghosts by I^- at pH 8.5. The sample was in 5 mM CHES buffer, pH 6.0, containing 3 mM KI. The temperature was 37 °C. (□) DEPC-modified EMA-labeled ghosts, mean triplet lifetime $1395(\pm 51)$ μ s; (○) control EMA-labeled ghosts, mean triplet lifetime $1423(\pm 47)$ μ s. (C) Quenching of DEPC-modified ghosts by TEMPO at pH 6.0. The sample was in 5 mM MES buffer, pH 6.0, containing 0.7 mM TEMPO. The temperature was 37 °C. (□) DEPC-modified EMA-labeled ghosts, mean triplet lifetime $1214(\pm 39)$ μ s; (○) control EMA-labeled ghosts, mean triplet lifetime $1189(\pm 45)$ μ s.

crystals of the transmembrane domain of band 3 was reported (30, 31). In the absence of an atomic resolution structure, however, spectroscopic methods provide a valuable approach to investigating the transport domain of band 3. We have previously obtained evidence that the eosin moiety of B3-EMA could be located in the wall of the anion access channel (16), although the EMA probe does not prevent substrate anions from binding to the transport pocket (8, 17). Thus, the study of the accessibility of charged molecules to B3-EMA should give insight into electrostatic properties in the vicinity of the anion transport site.

Macara et al. (9) investigated the fluorescence quenching of B3-EMA by Cs^+ and found that Cs^+ can only quench the fluorescence of B3-EMA from the cytoplasmic side of the membrane. They proposed that extracellular labeling of band 3 with EMA may change the protein conformation so that the eosin moiety becomes exposed to the intracellular space. More recently, Wyatt and Cherry (19) observed that I^- ions access B3-EMA from the extracellular side of the membrane. In the present report, we systematically investigated the sidedness effects of charged quenchers. The results from the quenching of B3-EMA in IOV and RSG samples indicate that the positively charged quenchers approach the eosin moiety from the cytoplasmic side of the erythrocyte membrane, whereas negatively charged quenchers approach from the extracellular side.

It follows from these findings that the eosin probe must be accessible from both sides of the membrane. This conclusion further supports our previous proposal that EMA binds to band 3 such that it is accessible via the anion transport pathway. Because the pathway is thought to consist of a thin barrier which is accessible from both sides of the membrane, it is quite feasible for the eosin probe to span this region of the protein. If EMA bound elsewhere on the protein, it is unlikely that it would be accessible from both sides. Since the eosin moiety of EMA is small (~ 0.7 nm) compared with the thickness of the membrane, this would require a major disruption of the transmembrane helices which are thought to surround the anion channel and the penetration of the aqueous medium deep into the protein.

The observation that for quenchers with the same charge, the bulkier quencher exhibits the smaller quenching rate constant, also suggests that the probe is accessed via a channel.

The effects of ionic strength and pH on the quenching reactions indicate that the collision of the quenchers with the eosin probe is influenced by electrostatic effects. It should be noted that unlike Cs^+ which quenches eosin fluorescence by a static mechanism (9) and thus presumably binds to band 3, the quenchers used in the present study all quench the eosin triplet state dynamically. It should also be pointed out that the iodide concentrations used to quench the triplet state are lower than those used in our previous study of fluorescence quenching where the Stern–Volmer plots were interpreted by a binding–diffusion model (16).

Electrostatic interactions can influence the rate constant for quenching by repulsion or attraction of the charged quenchers. Since the rate constant decreases with increasing ionic strength (which decreases electrostatic interactions) for both positively and negatively charged quenchers, we conclude that the electrostatic interaction is attractive in both cases. This can only occur if the positively and negatively charged quenchers approach the eosin probe by different paths, which is consistent with the finding that they act from opposite sides of the membrane.

Titration experiments were performed to investigate the nature of ionizable groups which might interact electrostatically with the quenchers. It was found that quenching decreased with increasing pH for negatively charged quenchers and increased with increasing pH for positively charged quenchers, with an apparent $pK_a \sim 6.5$ in both cases. This value of pK_a suggests the involvement of one or more histidine residues. Hamasaki et al. (32) have studied the participation of histidine residue(s) in band 3-mediated phosphate transport. They reported that the phosphate exchange rates were inhibited by DEPC in a dose-dependent manner with a half inhibition concentration of 1.5 mM. In the present study, we find that modification of band 3 by DEPC reduces the rate of quenching of EMA-B3 by I^- at pH 6 but not at pH 8.5, consistent with the loss of the

histidine ionizable group (33). Interestingly, although stilbenedisulfonate derivatives and DEPC are mutually exclusive in reacting with band 3 (22), prelabeling with EMA apparently did not inhibit the reaction with DEPC. This could be due to different binding of EMA and stilbenedisulfonates or because unsealed ghosts rather than RSGs were used for labeling in the present experiments.

Although the same histidine residue could conceivably influence quenching from both sides of the membrane, it seem much more likely that more than one histidine is involved. This proposal is strongly supported by the studies of Müller-Berger et al. (34, 35) who reported that substitution by site-directed mutagenesis of any one of the four histidine residues in the transmembrane domain of mouse erythroid band 3 inhibits Cl^- transport. From a hydrophobicity plot of band 3, these histidine residues are most likely located in the putative transmembrane helix 9 (His-721), helix 10 (His-752), helix 13 (His-852), and in the intracellular loop between helix 12 and 13 (36). It is also relevant to the present studies that those histidine residues are suggested to be located at different depths with respect to the membrane surface (34), as would be required for different histidines to influence the quenching reactions on opposite sides of the membrane.

A charged histidine residue in the vicinity of the eosin probe on the extracellular side of the membrane would contribute to the attractive electrostatic force experienced by negatively charged quenchers. Other positively charged residues such as arginines which might form the anion binding site could also contribute as they would remain ionized over the pH range investigated. On the cytoplasmic side, the attractive electrostatic force experienced by positively charged quenchers implies that the local net charge is negative. This could occur if the positive charge on a histidine residue is outweighed by the negative charge on the eosin probe itself and/or nearby anionic amino acids such as Glu (37). Such groups also would not be titrated over the pH range used for the quenching experiments.

In conclusion, the present studies in conjunction with our earlier investigation of fluorescence quenching of EMA-B3 by I^- , strongly indicate that the eosin probe is closely associated with the anion transport pathway of band 3. Our previous model requires modification to permit eosin to span the thin barrier which is thought to be the site of anion translocation. It is likely that there is a histidine residue in the vicinity of the eosin probe on either side of the membrane. Although labeling band 3 with EMA no doubt produces some structural perturbation, the finding that anion binding is little altered (8, 16, 18) encourages the view that such perturbation may be modest. Thus further spectroscopic studies with EMA-B3, particularly in conjunction with mutagenesis, can play a valuable role in elucidating properties of the anion transport pathway.

ACKNOWLEDGMENT

We thank Dr. P. O'Shea for helpful discussions and Dr. I.E.G. Morrison for help with instrumentation.

REFERENCES

- Low, P. S. (1986) *Biochim. Biophys. Acta* 864, 145–167.
- Jennings, M. L. (1985) *Annu. Rev. Physiol.* 47, 519–533.
- Kopito, R. R., and Lodish, H. F. (1985) *Nature* 316, 234–238.
- Tanner, M. J. A., Martin, P. G., and High, S. (1988) *Biochem. J.* 256, 703–712.
- Wood, P. G. (1992) in *The Band 3 Proteins; Anion Transporters, Binding Proteins and Senescent Antigens* (Bamberg, E., and Passow, H., Eds.) pp 325–352, Elsevier, Amsterdam.
- Salhany, J. M. (1990) *Erythrocyte Band 3 Protein*, CRC Press, Boca Raton, FL.
- Nigg, E. A., and Cherry, R. J. (1979) *Biochemistry* 18, 3457–3465.
- Liu, D., Knauf, P. A., and Kennedy, S. D. (1996) *Biophys. J.* 70, 715–721.
- Macara, I. G., Kuo, S., and Cantley, L. C. (1983) *J. Biol. Chem.* 258, 1785–1792.
- Tanner, M. J. A. (1993) *Semin. Hematol.* 30, 34–57.
- Cobb, C. E., and Beth, A. H. (1990) *Biochemistry* 29, 8283–8290.
- Passow, H., Lepke, S., and Wood, P. G. (1992) in *The Band 3 Proteins; Anion Transporters, Binding Proteins and Senescent Antigens* (Bamberg, E., and Passow, H., Eds.) pp 85–98, Elsevier, Amsterdam.
- Jennings, M. L. (1989) *Annu. Rev. Biophys. Biophys. Chem.* 18, 397–430.
- Passow, H. (1986) *Rev. Physiol. Biochem. Pharmacol.* 103, 61–203.
- Wood, P. G., Müller, H., Sovaka, M., and Passow, H. (1992) *J. Membr. Biol.* 127, 139–148.
- Pan, R. J., and Cherry, R. J. (1995) *Biochemistry* 34, 4880–4888.
- Liu, S. J., and Knauf, P. A. (1993) *Am. J. Physiol.* 264, C1155–C1164.
- Knauf, P. A., Strong, N. M., Penikas, J., Wheeler, R. P., Jr., and Liu, S. J. (1993) *Am. J. Physiol.* 264, C1144–C1154.
- Wyatt, K., and Cherry, R. J. (1992) *Biochemistry* 31, 4650–4656.
- Steck, T. L., and Kant, J. A. (1974) *Methods Enzymol.* 31, 172–180.
- Warren, L. (1963) *Methods Enzymol.* 6, 463–465.
- Izuhara, K., Okubo, K., and Hamasaki, N. (1989) *Biochemistry* 28, 4725–4728.
- Nigg, E. A., and Cherry, R. J. (1979) *Proc. Natl. Acad. Sci. USA* 77, 4702–4706.
- Cherry, R. J. (1978) *Methods Enzymol.* 54, 47–61.
- Eftink, M. R. (1991) in *Topics in Fluorescence Spectroscopy*, (Lakowicz, J. R., Ed.) Vol 2: pp 53–126, Plenum, New York.
- Errisson, U. G., Tozer, T. N., Sosnovsky, G., Lukszo, J., and Brasch, R. C. (1986) *J. Pharm. Sci.* 75, 334–337.
- Lagercrantz, C., Larsson, T., and Tollsten, L. (1985) *Biochem. Pharmacol.* 34, 31–38.
- Ross, A. H., and McConnell, H. M. (1975) *Biochemistry* 14, 2793–2798.
- Cherry, R. J. (1992) in *Structural and Dynamic Properties of Lipids and Membranes* (Quinn, P. J., and Cherry, R. J., Eds.) pp 137–152, Portland Press, London.
- Wang, D. N., Kuhlbrandt, W., Sarabia, V. E., and Reithmeier, R. A. F. (1993) *EMBO J.* 12, 2233–2239.
- Wang, D. N., Kuhlbrandt, W., Sarabia, V. E., and Reithmeier, R. A. F. (1994) *EMBO J.* 13, 3230–3235.
- Hamasaki, N., Izuhara, K., Okubo, K. (1989) in *Anion transport protein of the red blood cell membrane* (Hamasaki, N., and Jennings, M. L., Eds.) pp 47–59 Elsevier, Amsterdam.
- Miles, E. M. (1977) *Methods Enzymol.* 47, 431–442.
- Müller-Berger, S., Karbach, D., König, J., Lepke, S., Wood, P. G., Appelhans, H., and Passow, H. (1995a) *Biochemistry* 34, 9315–9324.
- Müller-Berger, S., Karbach, D., Kang, D., Aranibar, N., Wood, P. G., Ruterjans, H., and Passow, H. (1995b) *Biochemistry* 34, 9325–9332.
- Reithmeier, R. A. F. (1993) *Curr. Opin. Struct. Biol.* 3, 515–523.
- Jennings, M. L., and Smith, J. S. (1992) *J. Biol. Chem.* 267, 13964–13971.